Optimal Relay Selection and Power Allocation in an Improved Low-Order-Bit Quantize-and-Forward Scheme

Jianrong Bao [1,2], Dan He[1], Xiaorong Xu[1], Bin Jiang[1] and Minhong Sun[1,2]
[1] School of Communication Engineering, Hangzhou Dianzi University,
Hangzhou, Zhejiang, 310018-China
[E-mail: {baojr; 141080036; xuxr; jiangbin; cougar}@hdu.edu.cn]
[2] National Mobile Communications Research Laboratory, Southeast University,
Nanjing, Jiangsu, 210096-China,
*Corresponding author: Jianrong Bao

Received June 22, 2016; revised September 8, 2016; accepted September 25, 2016; published November 30, 2016

Abstract

Currently, the quantize-and-forward (QF) scheme with high order modulation and quantization has rather high complexity and it is thus impractical, especially in multiple relay cooperative communications. To overcome these deficiencies, an improved low complex QF scheme is proposed by the combination of the low order binary phase shift keying (BPSK) modulation and the 1-bit and 2-bit quantization, respectively. In this scheme, the relay selection is optimized by the best relay position for best bit-error-rate (BER) performance, where the relays are located closely to the destination node. In addition, an optimal power allocation is also suggested on a total power constraint. Finally, the BER and the achievable rate of the low order 1-bit, 2-bit and 3-bit QF schemes are simulated and analyzed. Simulation results indicate that the 3-bit QF scheme has about 1.8~5 dB, 4.5~7.5 dB and 1~2.5 dB performance gains than those of the decode-and-forward (DF), the 1-bit and 2-bit QF schemes, at BER of 10^{-2}, respectively. For the 2-bit QF, the scheme of the normalized Source-Relay (S-R) distance with 0.9 has about 5dB, 7.5dB, 9dB and 15dB gains than those of the distance with 0.7, 0.5, 0.3 and 0.1, respectively, at BER of 10^{-3}. In addition, the proposed optimal power allocation saves about 2.5dB much more relay power on an average than that of the fixed power allocation. Therefore, the proposed QF scheme can obtain excellent features, such as good BER performance, low complexity and high power efficiency, which make it much pragmatic in the future cooperative communications.

Keywords: Quantize-and-forward, low order quantization, low order modulation, relay selection, power allocation

This work was supported by the Zhejiang Provincial National Natural Science Foundation (No. LZ14F010003, No. LY15F010008), the National Natural Science Foundation of China (No. 61471152, No. 61271214), the Open Research Fund of National Mobile Communications Research Laboratory Southeast University (No. 2014D02), and the Zhejiang Provincial Science and Technology Plan Project(No. 2015C31103)

1. Introduction

In wireless communications, severe mutiple-path fading with time and frequency domain distortion easily occurs due to the phenomena such as transmission attenuation, shadowing and multi-path effect, and so on. To avoid these adverse impacts, diversity technique is put forward to compensate them. Recently, the well-known multiple-input multiple-output (MIMO) technique was proposed for space diversity and it was investigated to take advantage of the mutiple path effect as the independent signal component rather than the interference [1]. And the essential factor of a MIMO system is to exploit multiple transmit and receive antennas effectively to improve the spectrum efficiency and also the quality of service (QoS). However, mobile communication terminals, especially the widely used handset phones, are difficult to be equipped with multiple antennas. It is mainly due to the size limitation of the antenna arrays, which is not enough to produce independent signal components under the current licensed radio wavelength. So, a novel cooperative communication has been presented by using nearby communication nodes to relay messages and the cooperative space diversity can thus be obtained in the destination for a virtual MIMO system [2], [3]. After that, it has increasingly attracted much attentions as a feasible transmission strategies in the future wireless networks.

In cooperative communications, according to the mechanism of signal processing at the relay node, the cooperative strategies can be categorized as three main schemes such as: amplify-and-forward (AF), decode-and-forward (DF) and compress-and-forward (CF) and so on [4], [5]. Within the three schemes, the simplest AF scheme just amplifies both the signals and the noises without any performance gain, since it don't improve any signal-to-noise ratio (SNR). For the DF scheme, serious error propagation easily appeares when the channel quality between the source and relay is poor, which prohibites it far from being pragmatic. Due to the deficiency of the DF scheme, the CF scheme is proposed by quantizing, compressing and then forwarding the received signals from the relay node to the destination node. And it mainly utilizes the information correlation between the relay node and the destination node to compress the messages for good transmission efficiency. Nowadays, the investigations about the CF scheme are mainly generalized as two aspects. One is the Wyner-Ziv coding scheme, which has been used to compress and quantize the received signals [6]. Another is the simple quantization based quantize-and-forward (QF) without the consideration of the correlations [7]. Because the Wyner-Ziv coding is much more complex due to the huge information exchanges in the wireless networks, the much simpler QF scheme without the coding would be adopted and investigated in this paper. As a special case of the CF, the diversity gain of the QF is the same as that of the CF. For a typical two-hop relay system based on the QF protocol, it can achieve full diversity gains, *i.e.*, the diversity order is 2. Nowadays, there have been many studies about the QF scheme in literature as follows. For instance, the impact of modulation order and quantization order in the QF schemes were researched in [8] and [9]. And the conclusions were that higher quantization order led to better BER performance but it was accompanied by much higher computational complexity. Similarly, high modulation order had good transmission efficiency at the cost of decreased reliability. Due to high efficiency and low complexity of the QF scheme, it can obtain good transmission rate and thus be widely used in multiple-relay cooperative communications [10]-[12]. For the QF scheme, after being quantized, the received messages at the relay node is processed as the quantitative messages. And the messages are quantized to some sequences. Because the relaying messages for the QF are not the decoded messages or the amplified messages, which can avoid these problems in

the DF and AF schemes. For the 1-bit quantization, the quantization at the relay node is the same to perform hard decision. For the DF, the decoding at the relay node is to perform soft decision, which is superior to that of the 1-bit QF. But for the 2-bit or higher order bit QF, the received messages at the relay node are quantized as the 2 bit or the higher bit sequences, which allow the relay node to transmit much more available messages to the destination node. Although the hard decision is performed at the relay node, as well as the quantization errors, the QF scheme can even obtain good performance. In addition, higher order quantization order leads to higher computational complexity. So a moderate quantization order is needed in practice. Moreover, according to [8], the QF based relaying with M-ary phase shift keying (M-PSK) has been studied. Also, higher order modulation causes higher computational complexity. So, there is only the BPSK to be considered for the relay scheme. However, the proposed QF system model is also suitable for the general M-PSK modulation and the quadrature amplitude modulation (M-QAM). In addition, a low-density parity-check (LDPC) code with good performance can be adopted as the error protection code in each link [13].

In cooperative communications, relay selection and power allocation are two key issues. The relay selection is to choose the relay for best channel condition to relay the signals. Because only one relay works at each time slot, a strict time and carrier synchronization among the relays is not necessary for simplicity. Recently, there has been many relay selection strategies in cooperative communications based on AF and DF schemes [14]-[17]. To obtain good overall performance of a cooperative scheme, many factors should be taken into consideration. For instance, the instantaneous channel state information (CSI), outage probability (OP), signal-to-noise (SNR) boundary, bit error rate (BER), energy efficiency need to be evaluated. So in our proposed QF scheme, one relay is chosen with better channel location information to optimize the BER performance. Due to the practical limitation, the resource allocation is mainly focused on the power allocation. Then the optimal power allocation in the proposed QF scheme can be modeled as the general relay network to combat the time-varying fading channel states. And power allocation over channel state can produce new performance gains [18]. At present, there are mainly two power allocation methods, *i.e.*, the fixed and the optimal power allocation. The purpose of the latter is to find reasonable allocation and thus maximize the system power performance on a constrained total power. The optimal objectives mainly include maximal throughout, minimal BER, minimal symbol error rate, minimal outage probability, etc, [19]-[21]. In this paper, the throughout is also chosen as the measurement for the power allocation optimization. Therefore, relay selection and power allocation are optimized in the proposed QF scheme for good overall performance.

In this paper, a QF relay system based on relay selection with power allocation optimization is investigated. The main contributions of this paper are concluded as follows:

1) An improved QF protocol is proposed to solve the problem of high complexity in current QF relay systems;

2) Based on the proposed QF protocol, the relay with best CSI is optimally chosen;

3) The power allocation is optimized to achieve maximum throughout of a QF relay system.

The remainder of this paper is organized as follows. In Section 2, the relay system model and relay selection strategy based on the channel location information are introduced. According to the system model described in Section 2, an improved low bit and modulation order QF scheme is proposed at Section 3 for low complexity and good performance. Simultaneously, the quantization process at the relay node and the joint decoding at the destination node are depicted in detail. Based on the proposed QF scheme, an optimal power allocation method is also suggested and performed with theoretical analyses in Section 4. In

Section 5, numerical simulations and result analyses are presented to verify the good performance of the proposed QF scheme. Finally, the conclusion is drawn in Section 6.

2. Relay System Model and Relay Selection Strategy

2.1 Relay System Model

A typical 2-hop relay system is presented in **Fig. 1**. It consists of a source node (S), a destination node (D) and several relay nodes (R). Each node owns single and independent antenna, which causes the independent and identically distributed (*i.i.d.*), channel in the relay system. Since the relay system is usually characterized by half-duplex feature, here the time division half-duplex relay channel is considered to distinguish the different signals transmitted in the common channel. So, for a given transmission time, it is divided into two time slots.

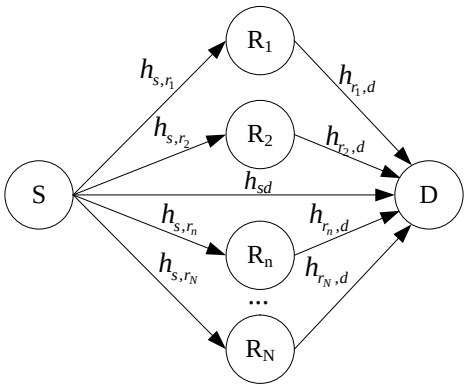

Fig. 1. The 2-hop relay system

In the first time slot (time slot-1), the source node broadcasts the first information part $\mathbf{x}_s^{(1)}$ to the *n*-th (*n*=1, …, *N*) relay nodes, as well as the destination node. And the signals received at the destination node and the *n*-th relay nodes are respectively as

$$\boldsymbol{y}_d^{(1)} = \sqrt{p_S^{(1)}} h_{sd} \boldsymbol{x}_s^{(1)} + \boldsymbol{n}_{sd} \ , \tag{1}$$

$$\boldsymbol{y}_{s,r_n} = \sqrt{p_S^{(1)}} h_{s,r_n} \boldsymbol{x}_s^{(1)} + \boldsymbol{n}_{s,r_n} , \tag{2}$$

where $\boldsymbol{y}_d^{(1)}$ and $\boldsymbol{y}_{s,r_n}$ are the received signals at the destination node and the *n*-th relay node, respectively. $\boldsymbol{x}_s^{(1)}$ and $p_S^{(1)}$ are the transmitted signal and the power at the source node in the time slot-1. h_{s,r_n} and h_{sd} are the channel coefficients of S-R and S-D links, respectively. $\boldsymbol{n}_{sd}$ and $\boldsymbol{n}_{s,r_n}$ are the complex additive white Gaussian noise (AWGN) with zero-mean and variances σ^2, corresponding with the S-D and S-R links.

In the second time slot (time slot-2), the messages received by the *n*-th relay node are quantized with the proposed scheme at first and then transmitted to the destination node. Simultaneously, the source node also transmits its second part information $\boldsymbol{x}_s^{(2)}$ to the destination node. Then, the received signal $\mathbf{y}_d^{(2)}$ at the destination node can be expressed as

$$\boldsymbol{y}_d^{(2)} = \sqrt{p_R} h_{r_n,d} \boldsymbol{x}_{r_n} + \sqrt{p_S^{(2)}} h_{sd} \boldsymbol{x}_s^{(2)} + \boldsymbol{n}_Q , \tag{3}$$

where $p_S^{(2)}$ and $\boldsymbol{x}_s^{(2)}$ are the transmitted power and signal at the source node in the time slot-2, respectively. P_R and $\boldsymbol{x}_{r_n}$ are the transmitted power and signal at the *n*-th relay node. $\boldsymbol{n}_Q$ is the complex AWGN with zero-mean and variances σ^2. $h_{r_n,d}$ is the channel coefficient (or gain) of the R-D link.

2.2 Relay Selection Strategy

A commonly used relay selection technique is based on the relay location information. Relay position can directly affect the performance of the relay systems. This is because the channel state information (CSI) with different relay position is different, which requires further determination to acknowledge the appropriate placement for the individual relay node.

As shown in **Fig. 1**, with many candidate relay nodes, an optimal relay node must be found to make the performance of a relay system best. Here the relay selection is optimized based on channel location information and the best relay position is correspondingly confirmed in the relay system.

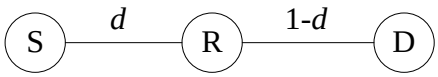

Fig. 2. The three-node relay system

In **Fig. 2**, suppose that the source node, the relay node and the destination node are located in a straight line. If the distance between the source and the destination node is normalized to 1, and the distance between the source and the relay node is supposed to be *d*, then the distance between the relay and the destination node is 1-*d*. For this case, we assume the normalized unit variance for the AWGN noise, and the Rayleigh fading effect as well. The fading and path loss are both merged into the indexes of the distance and the pass-loss for simplifying the system model [22]. Then, the signal-to-noise ratio (SNR) ($\gamma_{sd}^{(1)}$, $\gamma_{sd}^{(2)}$, γ_{sr}, γ_{rd}) of the S-D, S-R and R-D links are expressed as

$$\gamma_{sd}^{(1)} = |h_{sd}|^2 P_S^{(1)} = P_S^{(1)}, \tag{4}$$

$$\gamma_{sd}^{(2)} = |h_{sd}|^2 P_S^{(2)} = P_S^{(2)}, \tag{5}$$

$$\gamma_{sr} = |h_{sr}|^2 P_S^{(1)} = P_S^{(1)} / d^{\lambda}, \tag{6}$$

$$\gamma_{rd} = |h_{rd}|^2 P_R = P_R / (1-d)^{\lambda}, \tag{7}$$

where λ is the path-loss index ranging from 2 to 6. In this paper, it can be set as λ=2 for the typical free space environment [22]. Because only one relay node is chosen, these coefficients, $h_{r_n,d}$, h_{s,r_n}, $\boldsymbol{y}_{s,r_n}$, $\boldsymbol{x}_{r_n}$ and $\boldsymbol{n}_{s,r_n}$, are also writen as h_{rd}, h_{sr}, $\boldsymbol{y}_{sr}$, $\boldsymbol{x}_r$ and $\boldsymbol{n}_{sr}$.

According to the above analyses, the SNR of each link is mainly affected by the distance between each two terminal nodes of the link. Similarly, the BER performance of the relay system is determined by the SNR of each link. So an optimal relay node candidate need to be chosen with the proper relay position in the relay system for best BER performance.

3. The improved Quantize-and-Forward Scheme

According to the relay system model in **Fig. 1** and the related analyses, an improved low complex QF scheme is proposed as follows. According to the CF system model in [6], the

detailed block diagram of the QF relay system model is depicted in **Fig. 3**. And it mainly contains three parts, *i.e.*, the subplot (a) source node S, the subplot (b) relay node R and the subplot (c) destination node D, respectively. Also three proper low-density parity-check (LDPC) codes, namely, "LDPC-1", "LDPC-2" and "LDPC-3", are employed to meet the requirement of optimal cooperative transmission. Moreover, the low order BPSK modulator is used for modulating. Besides, because of the high complexity of Wyner-Ziv coding, the scalar quantizer is used for quantization. Next, the detailed process of the scheme will be discussed.

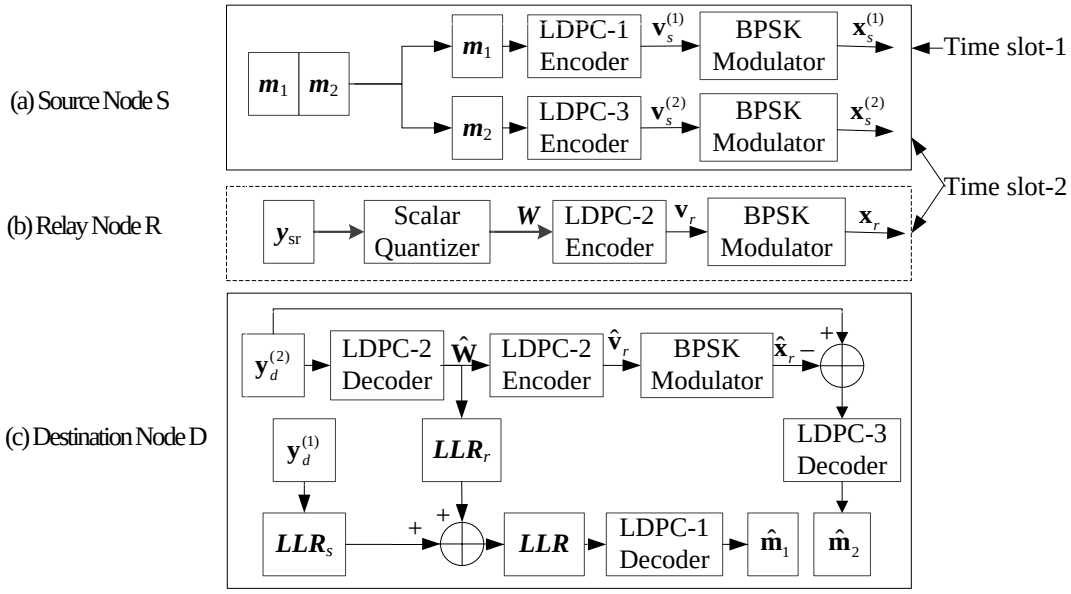

Fig. 3. Block diagram of the improved QF scheme.

1) At the source node of **Fig. 3(*a*)**, the source information bit sequence are divided into two information parts. The first part $\boldsymbol{m}_1$ are encoded with the LDPC-1 encoder, and the code word $\boldsymbol{v}_s^{(1)}$ are generated. Then, the BPSK modulated signals $\boldsymbol{x}_s^{(1)}$ are produced after a BPSK modulator. Finally, $\boldsymbol{x}_s^{(1)}$ are broadcasted to the relay and the destination nodes in the time slot-1, respectively. For the second part $\boldsymbol{m}_2$, they are encoded with the LDPC-3 encoder, and the code word $\boldsymbol{v}_s^{(2)}$ is thus obtained. After BPSK modulation, the signals $\boldsymbol{x}_s^{(2)}$ are transmitted to the destination node in the time slot-2.

2) For the chosen relay node as described in **Fig. 3(*b*)**, the scalar quantizer is applied to quantize the received signals after receiving the information $\boldsymbol{y}_{sr}$. Subsequently, the quantized information sequence $\boldsymbol{W}$ are encoded by the LDPC-2 encoder. Then, the code word $\boldsymbol{v}_r$ is obtained. After the BPSK modulation, the signals $\boldsymbol{x}_r$ are transmitted to the destination node.

3) At the destination node of **Fig. 3(*c*)**, in order to achieve the whole source information $\boldsymbol{m}$, two main decoding processes are analyzed as follows.

a) One is the restoration of the first part information. For the received information at the destination node in time slot-2, it contains two part, *i.e.*, $\hat{\boldsymbol{x}}_s^{(2)}$ and $\hat{\boldsymbol{x}}_r$, respectively. After LDPC-2 decoding, the decoded quantization information $\hat{\boldsymbol{W}}$ and code word $\hat{\boldsymbol{v}}_s^{(2)}$ are obtained jointly. Then, the quantization information $\hat{\boldsymbol{W}}$ from $\boldsymbol{y}_d^{(2)}$ is extracted. Subsequently, it is

combined with the received information $\boldsymbol{y}_d^{(1)}$ in the time slot-1 by the maximal rate combining (MRC) strategy to recover the first part of the source message $\hat{\boldsymbol{m}}_1$. By transmitting the quantized information instead of the decoded information, the MRC at the destination node is improved by the combination of the log-likelihood ratio (LLR) values. The detailed jointly decoding is described in Subsection 3.2.

b) Another is the restoration of the second information part. By removing $\hat{\boldsymbol{x}}_r$ from $\boldsymbol{y}_d^{(2)}$, the rest part is the $\hat{\boldsymbol{x}}_s^{(2)}$, and the second part of the source information $\hat{\boldsymbol{m}}_2$ can be obtained by the LDPC-3 decoding.

In the QF scheme, the LDPC codes are the candidate of the proper channel code words used in this cooperation. In order to distinguish the LDPC codes at each node, three type of the LDPC codes are introduced. The LDPC codes at source node are named as LDPC-1 and LDPC-3, respectively. They are used to encode the first information part $\boldsymbol{m}_1$ and the second information part $\boldsymbol{m}_2$, respectively. And also, the LDPC-2 code is adopted at the relay node. It is used to encoder the quantization information. So it is closely related with the quantization order and its length grows with the quantization order. Take 1-bit and 2 bit for example, the code length of the LDPC-2 code is the same or twice as that of the LDPC-1 codes.

Besides, the proportion of $\boldsymbol{m}_1$ and $\boldsymbol{m}_2$ in $\boldsymbol{m}=\boldsymbol{m}_1+\boldsymbol{m}_2$ affect the performance of the QF relay system. The channel utilization coefficient is defined as $\beta=\boldsymbol{m}_1/\boldsymbol{m}$. Generally, larger coefficient results in higher reliability, also inferior effectiveness. So a appropriate channel utilization value is needed.

In order to achieve better performance, the LDPC code construction, scalar quantizer design, joint decoding analyses and etc, should be paid more attentions. The LDPC code is first introduced in reference [13], where the basic encoding and decoding algorithm are listed. Based on these results, the code construction algorithms proposed in reference [23] are used here to construct each LDPC codes. And the scalar quantizor and joint decoding are analyzed in Subsection 3.1 and Subsection 3.2, respectively.

3.1 Scalar Quantization at the Relay Node

To reduce the quantization complexity, a low complex scalar quantization is adopted in the proposed scheme [24]. As described in **Fig. 3**, the input signal of the scalar quantizer is assumed as $\boldsymbol{y}_{sr}$. After scalar quantization, each element in the vector $\boldsymbol{y}_{sr}$ is quantized as a binary sequence $\mathbf{Q}_{sr}=(q_{sr,1},...,q_{sr,M})$, where the quantization order is 2^M. The design purpose of the scalar quantizer is to determine the optimal quantization interval boundaries with a certain criterion, *i.e.*, to compute the values of $D_0,...,D_i,...,D_{2^M}$, where $0<i<2^M$. According to these quantization boundaries, each element in the vector $\mathbf{y}_{sr}$ is quantized according to the corresponding quantization interval. And the specific quantization process is described in detail as follows.

For each element in the vector $\boldsymbol{y}_{sr}$, if $D_{i-1}<y_{sr,j}<D_i$, $y_{sr,j}$ is mapped to a binary sequence $\boldsymbol{W}_i$. It can be written as

$$Q_{sr,j}=F(y_{sr,j})=\boldsymbol{W}_i, D_{i-1}<y_{sr,j}<D_i, \tag{8}$$

where $F(\cdot)$ is quantization function, $y_{sr,j}$ and $Q_{sr,j}$ are the j-th element in vector $\boldsymbol{y}_{sr}$ and $\boldsymbol{Q}_{sr}$. j is an integer greater than or equal to 1. And it is also less than or equal to the total number of the vector $\boldsymbol{y}_{sr}$.

Take a 2-bit scalar quantization for example, there are 5 quantization interval and 4 quantization results, *i.e.*, the quantization order is 4. According to Equation (8), the quantization boundaries are assume to be D_0, D_1, D_2, D_3, D_4 , respectively. Then, the binary sequences are induced as follows.

For the case $D_0<y_{sr,j}<D_1$, the quantization information is $\boldsymbol{W}_1$=00. For the other cases as $D_1<y_{sr,j}<D_2$, $D_2<y_{sr,j}<D_3$ and $D_3<y_{sr,j}<D_4$, there are $\boldsymbol{W}_2$=01, $\boldsymbol{W}_3$=10 and $\boldsymbol{W}_4$=11, respectively.

Due to the symmetry property of the modulation signals, the quantizaion boundaries can be reasonably assigned as

$$D_0=-\infty, D_4=\infty, D_2=0, D_1=D_3=D. \tag{9}$$

In Equation (9), there is only one unknown number *D*. It is possible to obtain the optimal value *D* based on the quantization criterion. The general criterion is to maximize the quantization sequence information, which is equivalent to minimize the entropy of symbol $y_{sr,j}$ with the output $Q_{sr,j}$.

For other order quantization, it can be similarly extended and analyzed just as the case of the 2-bit quantization mentioned above. So there will be no tautology.

3.2 Joint Decoding at the Destination Node

After receiving the quantization signals from R-D link and the signals from S-D link in the time slot-2, the destination node performs LDPC-2 channel decoding. So the decoded quantization information $\hat{\boldsymbol{W}}$ and code word $\hat{\boldsymbol{v}}_s^{(2)}$ are generated. By LDPC-3 decoding of the message part $\hat{\boldsymbol{v}}_s^{(2)}$, the second information part $\hat{\boldsymbol{m}}_2$ can be produced. Meanwhile, the message part $\hat{\boldsymbol{W}}$ and $\mathbf{y}_d^{(1)}$ are jointly performed with MRC computation, and the first information part $\hat{\boldsymbol{m}}_1$ is also obtained.

For the recovery of the first information part, the joint decoding is adopted at the destination node for better reliable decoding. And the MRC at the destination node is improved by the combination of the log-likelihood ratio (LLR) values. The input LLR of LDPC-1 decoder is the sum of $\boldsymbol{LLR}_s$ and $\boldsymbol{LLR}_r$, and it is

$$\boldsymbol{LLR}=\boldsymbol{LLR}_s+\boldsymbol{LLR}_r, \tag{10}$$

where $\boldsymbol{LLR}_s$ and $\boldsymbol{LLR}_r$ are the LLR values of the S-D and R-D links, respectively. For the irerative decoder for an LDPC code, the iterative decoding is performed by passing messages between the variable-node decoder (VND) and variable-node decoder (CND) [25].

For the VND, Suppose that a variable node of degree d_v has d_v+1 incoming messages, d_v from the edge interleaver and another one from the channel. Then the messages in the variable nodes are calculated by

$$L_{s,out}=L_{ch}+\sum_{s\neq t}L_{t,in} \qquad s,t=1,2,...,d_v, \tag{11}$$

where $L_{t,\text{in}}$ is the *t*-th priori LLR value input into the variable node, $L_{s,\text{out}}$ is the *s*-th extrinsic LLR value output of the variable node, and L_{ch} is the LLR value received from the channel.

For the CND, suppose the decoding of a degree d_c check node corresponds to the decoding of a length d_c single parity-check code. The output LLR values are

$$L_{s,out}=\ln[(1-\prod_{s\neq t}\frac{1-e^{L_{t,in}}}{1+e^{L_{t,in}}})/(1+\prod_{s\neq t}\frac{1-e^{L_{t,in}}}{1+e^{L_{t,in}}})]. \tag{12}$$

After receiving the extrinsic messages at the VNDs and CNDs, the log-likelihood-ratio based belief-propagation (LLR-BP) decoding is performed.

For the received information $\boldsymbol{y}_d^{(1)}$ at the destination node in the time slot-1, the LLR calculation of it is same as the general belief propagation (BP) algorithm [13]. For the BPSK modulation signal x, the LLR_s of each element in vector $\boldsymbol{y}_d^{(1)}$ is calculated as

$$LLR_s = \ln\left[p(x=1|y_d^{(1)}) / p(x=-1|y_d^{(1)}) \right]. \tag{13}$$

For the quantization information $\hat{\boldsymbol{W}}$, it is generated by the 2-bit quantization. Then one element is denoted by a 2-bit binary sequence, and there are

$$\begin{aligned} LLR_r &= \ln[\, p(\boldsymbol{W}_i|x=1) / p(\boldsymbol{W}_i|x=-1)] \\ &= \ln\left(\frac{\int_{D_{i-1}}^{D_i} p(y|\boldsymbol{W}_i=10)dy + \int_{D_{i-1}}^{D_i} p(y|\boldsymbol{W}_i=11)dy}{\int_{D_{i-1}}^{D_i} p(y|\boldsymbol{W}_i=00)dy + \int_{D_{i-1}}^{D_i} p(y|\boldsymbol{W}_i=01)dy} \right), \end{aligned} \tag{14}$$

where (D_{i-1}, D_i) is the corresponding quantization interval of the quantization information $\boldsymbol{W}_i$.

Without considering the side information from $\boldsymbol{y}_d^{(1)}$ for the quantization of $\boldsymbol{y}_{sr}$, the transition probability from $\boldsymbol{x}_s^{(1)}$ to $\boldsymbol{W}$ is

$$\begin{aligned} p(\boldsymbol{W}=\boldsymbol{W}_i|x=x_{s,k}^{(1)}) &= \int_{D_{i-1}}^{D_i} p(y|x=x_{s,k}^{(1)})dy \\ &= \frac{1}{\sqrt{2\pi}} \int_{D_{i-1}}^{D_i} \mathrm{e}^{-(y-y_{sr,j})^2/2} dy \end{aligned} . \tag{15}$$

If $x_{s,k}^{(1)} = -1$, and $D_0 < y_{sr,j} < D_1$, the quantization information is $\boldsymbol{W}_1$=00, where $x_{s,k}^{(1)}$ is the k-th element in vector $\boldsymbol{x}_s^{(1)}$, and k is greater than or equal to 1, and less than or equal to the total number of vector $\boldsymbol{x}_s^{(1)}$. According to Equation (15), the transition probability can be computed as

$$\begin{aligned} p(\boldsymbol{W}=\boldsymbol{W}_1|x=-1) &= \frac{1}{\sqrt{2\pi}} \int_{D_0}^{D_1} \mathrm{e}^{-(y+\sqrt{p_S^{(1)}}h_{sr})^2/2} dy \\ &= 1 - Q(\sqrt{p_S^{(1)}}h_{sr} + D_1) \end{aligned} , \tag{16}$$

where $Q(\cdot)$ function is $Q(x) = \frac{1}{\sqrt{2\pi}} \int_x^{\infty} \exp(-y^2/2) dy$.

According to Equation (16), all LLR values of the quantization information can be achieved. Take $\boldsymbol{W}_1$=00 for instance, the quantization interval is (D_0, D_1). Then the LLR value can be denoted as

$$\begin{aligned} &\ln[\, p(\boldsymbol{W}_1|x=1) / p(\boldsymbol{W}_1|x=-1)] \\ &= \ln\left[Q(\sqrt{p_S^{(1)}}h_{sr} - D_1) / (1 - Q(\sqrt{p_S^{(1)}}h_{sr} + D_1)) \right]. \end{aligned} \tag{17}$$

Similarly, if $\boldsymbol{W}_2$=01, the quantization interval of it is (D_1, D_2), and the LLR value of it is

$$\begin{aligned} &\ln[\, p(\boldsymbol{W}_2|x=1) / p(\boldsymbol{W}_2|x=-1)] \\ &= \ln \frac{Q(D_1 - \sqrt{p_S^{(1)} p_s}h_{sr}) - Q(D_2 - \sqrt{p_S^{(1)}}h_{sr})}{Q(D_1 + \sqrt{p_S^{(1)}}h_{sr}) - Q(D_2 + \sqrt{p_S^{(1)}}h_{sr})}. \end{aligned} \tag{18}$$

In summary, the LLR calculation of each $\boldsymbol{W}_i$ is generalized as

$$\ln[p(\boldsymbol{W}_i|x=1)/p(\boldsymbol{W}_i|x=-1)] = \ln\frac{Q(D_{i-1}-\sqrt{p_S^{(1)}}h_{sr})-Q(D_i-\sqrt{p_S^{(1)}}h_{sr})}{Q(D_{i-1}+\sqrt{p_S^{(1)}}h_{sr})-Q(D_i+\sqrt{p_S^{(1)}}h_{sr})}. \quad (19)$$

According to Equation (19), the LLR values of the remainder two cases can be obtained. When $\boldsymbol{W}_3$=10, the quantization interval of it is (D_2, D_3), and the LLR value of it is

$$\ln[p(\boldsymbol{W}_3|x=1)/p(\boldsymbol{W}_3|x=-1)] = \ln\frac{Q(D_2-\sqrt{p_S^{(1)}}h_{sr})-Q(D_3-\sqrt{p_S^{(1)}}h_{sr})}{Q(D_2+\sqrt{p_S^{(1)}}h_{sr})-Q(D_3+\sqrt{p_S^{(1)}}h_{sr})}. \quad (20)$$

When $\boldsymbol{W}_4$=11, the quantization interval of it is (D_3, D_4), and the LLR value of it is

$$\ln[p(\boldsymbol{W}_4|x=1)/p(\boldsymbol{W}_4|x=-1)] = \ln\frac{Q(D_3-\sqrt{p_S^{(1)}}h_{sr})-Q(D_4-\sqrt{p_S^{(1)}}h_{sr})}{Q(D_3+\sqrt{p_S^{(1)}}h_{sr})-Q(D_4+\sqrt{p_S^{(1)}}h_{sr})}. \quad (21)$$

For other higher or lower quantization order, the analyses are the same as described in Subsection 3.2. So, for conciseness, no more tautology will be discussed here.

4. Optimal Power Allocation of QF Scheme

For the proposed QF scheme, at the quasi-static Rayleigh channel, the channel state information (CSI) of each link is supposed to be achieved. So, for the time division half-duplex channel, the maximum achievable rate can be calculated. According to the results in [26] and the analyses from Equation (1) to Equation (3), the maximum theoretical achievable rate of the proposed scheme is derived as

$$R_{QF} = \frac{\beta}{2}\log(1+c_1p_S^{(1)}+\frac{c_2p_S^{(1)}}{1+T})+\frac{1-\beta}{2}\log(1+c_1p_S^{(2)}), \quad (22)$$

where T is

$$T = \frac{c_1p_S^{(1)}+c_2p_S^{(1)}+1}{((1+c_3p_R/(1+c_1p_S^{(2)}))^{(1-\beta)/\beta}-1)(1+c_1p_S^{(1)})}. \quad (23)$$

In Equation (22) and Equation (23), these coefficients are $c_1=|h_{sd}|^2$, $c_2=|h_{sr}|^2$ and $c_3=|h_{rd}|^2$, respectively. If all nodes have known CSI, the channel coefficients are determined. Assume that the source node transmits signal with power $P_S=P_S^{(1)}+P_S^{(2)}$ regardless of the channel state, where $P_S^{(1)}=\beta P_S$ and $P_S^{(2)}=(1-\beta)P_S$, β can be set as 1/2. Moreover, the relay node can adjust the power P_R adaptively with respect to the channel state information (CSI) in each information block. According to these assumptions and the corresponding analyses, Equation (22) can be finally concluded and rewritten as

$$R_{QF} = \frac{1}{4}\log(1+\frac{1}{2}c_1P_S+\frac{c_2c_3P_SP_R}{2+c_1P_S+c_2P_S+2c_3P_R})+\frac{1}{4}\log(1+\frac{1}{2}c_1P_S). \quad (24)$$

According to Equation (24), the optimal power allocation $P_{opt.}$ can be calculated as

$$P_{opt.} = \arg\max_{P_R} R_{QF}, \tag{25}$$

where P_R subjects to

$$P_R = P - P_S, \tag{26}$$

and P is set as the total power constraint. According to the optimal objective and the constraint, the above problems can be solved by the Lagrange multiplication method. Consider the Lagrange function as

$$L(P_R) = R_{QF}(P_R) - \mu(P_R - P). \tag{27}$$

Set $\frac{\partial L(P_R)}{\partial P_R} = 0$, then there is

$$R'_{QF}(P_R) - \mu = 0. \tag{28}$$

Define new objective function for the optimization as

$$g(P_R) = 1 + \frac{1}{2} c_1 P_S + \frac{c_2 c_3 P_S P_R}{2 + c_1 P_S + c_2 P_S + 2 c_3 P_R}. \tag{29}$$

Then, the first and the second derivative of Equation (29) are deduced as

$$g'(P_R) = \frac{c_1 c_2 P_S (2 + c_1 P_S + c_2 P_S)}{(2 + c_1 P_S + c_2 P_S + 2 c_3 P_R)^2}, \tag{30}$$

$$g''(P_R) = \frac{-4 c_1 c_2 c_3 P_S (2 + c_1 P_S + c_2 P_S)}{(2 + c_1 P_S + c_2 P_S + 2 c_3 P_R)^3}. \tag{31}$$

According to the composition law of concavity [27], the QF rate R_{QF} is concave with respect to P_R. According to Equation (24) and Equation (30), it is straightforward to get

$$R'_{QF}(P_R) = \frac{g'(P_R)}{4 g(P_R) \ln 2} = \frac{c_1 c_2 P_S (2 + c_1 P_S + c_2 P_S)}{4 g(P_R) \ln 2 (2 + c_1 P_S + c_2 P_S + 2 c_3 P_R)^2}. \tag{32}$$

Combine Equation (28) and Equation (32) together, there is

$$g(P_R)(2 + c_1 P_S + c_2 P_S + 2 c_3 P_R)^2 = \frac{c_1 c_2 P_S (2 + c_1 P_S + c_2 P_S)}{4 \mu \ln 2}. \tag{33}$$

Then the optimization problem is equivalent to the solution of Equation (33). Due to the high complex relationship of the related parameters, the closed-form solution can't be obtained. So the numerical calculation similar to reference [18] can be used to solve Equation (33).

Based on the above optimal power allocation, the relay selection can be described and analyzed again. Similar to the description in Section 2, the difference is the power value in Equation (5) and Equation (6), the transmitted power P_R at the selected relay node is just the solution of Equation (33). And the transmitted power at the source node is the same with that in Section 2.

In summary, for the proposed low-order-bit QF scheme, it features the same to that of the CF scheme. Simultaneously, it can realize effective relay with low complexity. By scaling with the optimal power allocation, the QF relay system can not only save the power resource, but also improve the BER performance of the whole QF relay system in cooperative communications.

5. Numerical Results and Analysis

To verify the effectiveness of the proposed QF scheme, the BER performance, the achievable rate by the power allocation are simulated and compared with the contrast schemes. According to the relay system model in **Fig. 1**, the simulation parameters are set as follows. The channels between alternative two nodes in the relay system are Rayleigh fading and AWGN. The variance of the fading channel coefficient is set as 1 for concise simulation processing. The AWGN parameters are the same for each link with zero mean and variance 1. The BPSK modulation and the LDPC codes are employed in the scheme. According to the requirement in the QF system model of **Fig. 3**, the LDPC codes are constructed by the method in [23]. And the max iteration in the Monte Carlo simulation of LDPC decoding is set as 50 in each SNR simulation point. Since there is two case of the code applications, they can be constructed by the parameters as follows.

1) For the situation "m_2=0", *i.e.*, the source node is idle in the time slot-2, and the LDPC-1 and LDPC-2 codes are needed to be constructed. For the 3-bit QF, the code length of the LDPC-2 code is three times as that of the LDPC-1 code. The code rates of the two LDPC codes are both 1/2, and the code length are 1000 and 6000, respectively. For the 2-bit QF, the code length of LDPC-2 code is twice as that of the LDPC-1 code. The code rates of the two LDPC codes are both 1/2, and the code length are 1000 and 4000, respectively. For the 1-bit QF scheme, the code length at the source node is the same to that at the relay node. And the same LDPC codes are used here. In short sumary, LDPC-1 code is the same to that of the LDPC-2 code, and they are also the same in the 2-bit QF scheme.

2) For the situation "m_1=m_2", the parameters of the LDPC-1 code is the same to that of the LDPC-3 code. In the 3-bit QF scheme, for the purposed of comparison, the code rate of the LDPC-1 and the LDPC-2 codes are both set as 1/2. And the code lengths of them are 500 and 3000, respectively. In the 2-bit QF scheme, for the purposed of comparison, the code rate of LDPC-1 and LDPC-2 codes are both set as 1/2. And the code length of them are 500 and 2000, respectively. In the 1-bit QF scheme, the three LDPC codes are constructed similarly. And only the LDPC-1 code is constructed the same to that of the 2-bit QF scheme.

Based on the above analyses, the three nodes are supposed to be located equidistant. Then, the BER performance of the 1-bit, 2-bit and 3-bit QF schemes along with the situation of m_2=0 and m_1=m_2 are simulated and given in **Fig. 4**, respectively.

Fig. 4 indicates that the proposed 3-bit QF has better BER performance than that of the 1-bit and 2-bit QF scheme. In the case of m_2=0, at BER of 10^{-2}, it obtains about 7.5dB and 2.5dB performance gains, respectively. In the case of m_1=m_2, at BER of 10^{-2}, it obtains about 4.5dB and 1dB performance gains, respectively. The reason is that the hard decision is performed at the relay node for the 1-bit QF, and for higher order QF, the quantize process makes more received information at the relay node to be transmitted to the destination node, which improves the BER performance much better.

According to the above simulation results and analyses, the higher order quantization is superior to low order quantization. But for the cost, the complexity of the former is also increased with the growth of the quantization order. Then, for the proposed QF scheme, the complexity of the scalar quantization is thus analyzed here. Firstly, for the calculation of quantization boundaries, there is only 1 variable needed to be computed for the 2-bit QF scheme, and no variable for the 1-bit QF one. But for the 3-bit QF scheme, there are 3 boundaries needed to be calculated. So, higher quantization order surely results in higher computational complexity. Secondly, the code length at the relay

node is proportional to the quantization information length. The encoding and decoding complexity of the code is proportional to the code length. Finally, at the destination node, the jointly decoding is adopted. To achieve the LLR value of one bit information, there are 1 multiplication operation for 1-bit QF scheme, 2 additive operations and 1 multiplication operation for the 2-bit QF scheme. But for the 3-bit QF scheme, there are 6 additive operations and 1 multiplication operation. However, for the CF relay system in [6], at the relay node, the nested quantizer and the distributed joint source-channel (DJSC) encoder are employed. At the destination node, the estimator is used to restore the quantization information. The computational complexity of the proposed QF scheme is still smaller than that of the CF scheme. Therefore, the trade off of the implementation complexity and performance should be chosen to obtain a reasonable quantization order in practice.

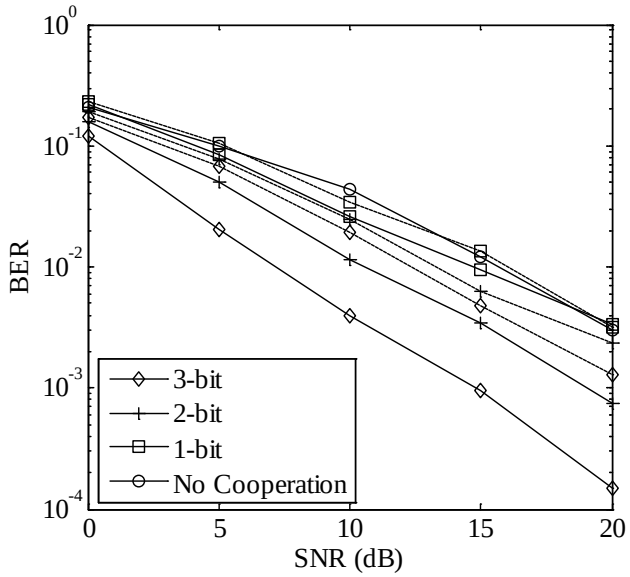

Fig. 4. The BER of the QF schemes. The solid lines represent the corresponding QF in situation m_2=0, and the dotted lines are for the situation m_1=m_2.

According to the definition of channel utilization coefficient β, there are β=1 in the case m_2=0, and β=1/2 in the case m_1=m_2, respectively. As described in Section 2, larger channel utilization coefficient leads to higher reliability. And the transmission efficiency generally compromises with the reliability of the two parameters, *i.e.* better one leads to worse another or vise versa. From **Fig. 4**, the BER performance of the QF scheme in the case m_2=0 is better than that of the case m_1=m_2. For the 1-bit, 2-bit and 3-bit QF schemes, at BER of 10^{-2}, there are 1dB, 4.5dB and 6dB performance gains, respectively, which provides strong supports for the above analyses. Therefore, the system can select the appropriate value of β for the compromise of the reliability and efficiency.

For case m_2=0, some typical relay schemes are given to make the comparison. With the same simulation parameters used for **Fig. 4**, the BER performance of each relay scheme is simulated and shown in **Fig. 5**.

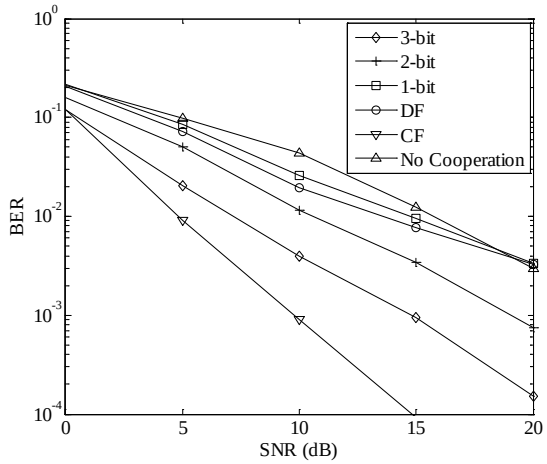

Fig. 5. The BER of different relay schemes.

Fig. 5 indicates that the proposed 3-bit QF has better BER performance than that of the 1-bit, 2-bit QF and DF schemes. At BER of 10^{-2}, it obtains about 7.5dB, 2.5dB and 5dB performance gains, respectively. The reason is that the hard decision is performed at the relay node for the 1-bit QF, and the belief propagation (BP) decoding occurs at the relay node for the DF scheme. But all these QF relay schemes perform worse than the CF scheme. This is because that the side information is not taken into consideration in the QF scheme. According to the above analyses, the computational complexity of the CF scheme is much larger than that of the QF scheme. So the proposed QF scheme obtains lower complexity at the cost of a little BER performance loses.

From the above simulation result, the BER performance of the case m_2=0 is superior to that of the case m_1=m_2. And the 3-bit QF scheme has better BER performance than the 1-bit and 2-bit QF scheme. Considering the computational complexity and BER performance together, the 2-bit QF is analyzed in following simulations. As described in Section 2, the channel location information also plays an important role in the final performance of the proposed scheme. Then, the relay selection based on the channel location information is also simulated and shown in **Fig. 6**. It gives the BER performance of the 2-bit QF scheme in different S-R distance of the case m_2=0 .

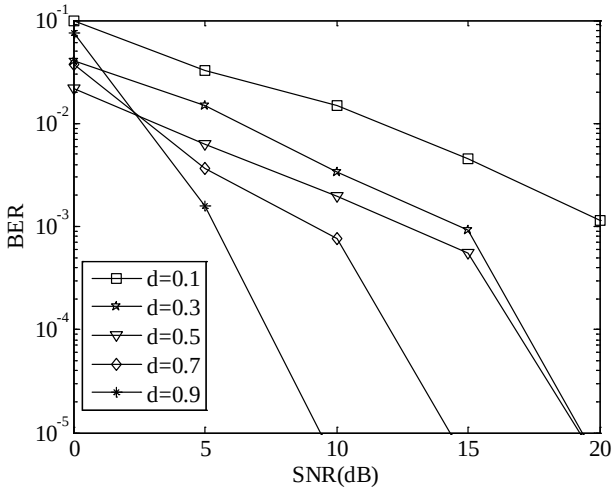

Fig. 6. The BER of the QF schemes with different S-R distance.

In **Fig. 6**, the BER performance of the 2-bit QF scheme grows with the decreased distance between the source node and the relay node. When the S-R distance increases and the R-D distance decreases, the BER performance get improved. For the 2-bit QF scheme, the scheme of S-R distance of 0.9 has about 5dB, 7.5dB, 9dB and 15dB gains than that of the distance of 0.7, 0.5, 0.3 and 0.1, respectively, at BER of 10^{-3}. This is because that the QF scheme performs no hard decision and thus has no error propagation phenomenon. So the information distortion, usually appeared in the DF scheme, can be avoided. And the quantization procedure makes the received information at the relay node to be sent to the destination node as much as possible. So shorter distance between relay and destination leads to lower error probability, *or* better BER performance. Therefore, in the multi-branch relay system, the relay located nearly to the destination node can obtain much better performance than other contrast cases.

Besides the performance and complexity, the channel capacity of the improved QF scheme is also simulated and analyzed. According to Equation (4)~(7) and Equation (22), the power at each node is shown by the corresponding SNR. The channle coefficients h_{sd} , h_{sr} and h_{rd} are both set as 1, *i.e.*, $E(|h_{sd}|^2)=1$, $E(|h_{sr}|^2)=1$ and $E(|h_{rd}|^2)=1$. Therefore, in the simulations, for the achievable rate of a relay system with the QF scheme, the transmitted power at the source and the relay nodes are all chosen as $P_{s,1}=P_{s,2}$=SNR and P_R=SNR/(1-β), respectively, where β is assumed as 1/2. In this case, the power at the relay node is the same to that at the source node. Then the achievable rate of each scheme is simulated and shown in **Fig. 7**.

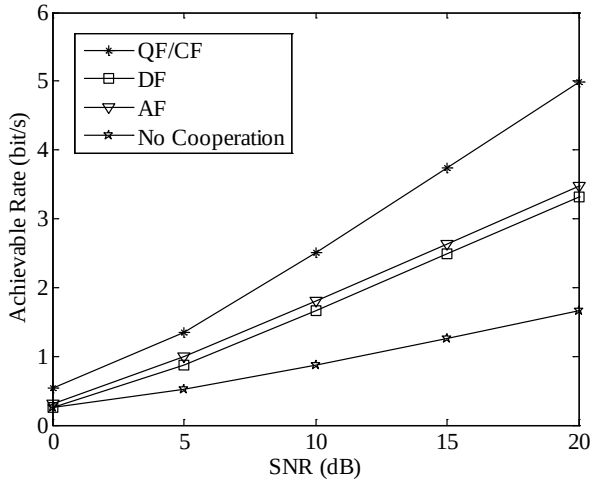

Fig. 7. The achievable rate of the cooperative schemes.

According to Equation (22) in the above analyses and Equation (15) in reference [5], the achievable rate of the QF and CF schemes are equal when the coefficient $\alpha=\beta$. **Fig. 7** also shows that the QF scheme has a rather large advantage over that of the DF scheme at high SNR. Moreover, the achievable rate of the QF and CF schemes are almost the same. And they are unconstrained by the S-R channel capacity for the QF scheme. So the QF scheme obtains a best practicality among these cooperative schemes .

For the optimal power allocation described in Section 4, where P_R are obtained by the Equation (33) in Section 4, and P_S is set the same to that of the fixed constant power allocation. In the fixed constant power allocation, the transmission power of each node is all set as $P_{s,1}=P_{s,2}= P_R =1/3P$. By the above simulation parameters, the numerical experiment results are shown in **Fig. 8**.

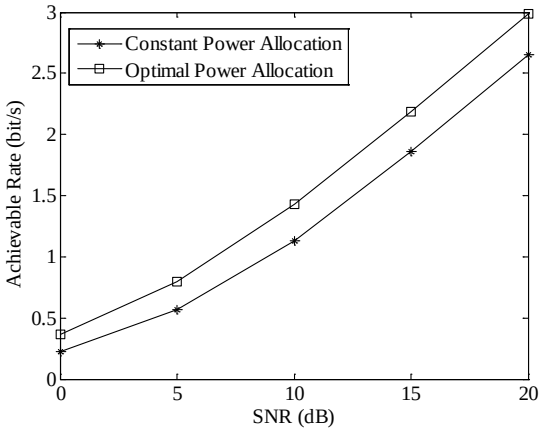

Fig. 8. The achievable rate by the optimal power allocation.

Fig. 8 indicates that the optimal power allocation solution brings significant rate gains at the same SNR, when compared with the fixed constant power allocation. In particular, using the QF scheme, it saves about 2.5dB relay power on average. This reflects the significance of the relay power allocation and the effectiveness of the analyzed solution. But also, as it described in Section 4, it is indispensable to compute the optimal relay power. So the optimal power allocation algorithm can achieve extra rate gains at the expense of high computational complexity.

Based on the above analyses, the relay selection with optimal power allocation is simulated and shown in **Fig. 9**. As analyzed in Section 2 and Section 4, the good features of the improved QF scheme are also verified by the numerical simulations .

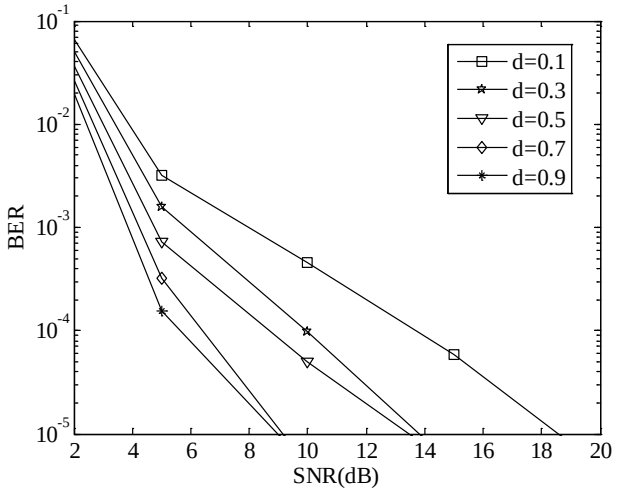

Fig. 9. The BER of the QF scheme in different S-R distance with optimal power allocation.

In **Fig. 9**, the BER performance of the QF relay system increases with the distance between the source and relay node. With the scheme of S-R distance of 0.9, it has about 0.8dB, 3 dB, 4dB and 8dB gains, respectively, when compared with that of S-R distance of 0.7, 0.5, 0.3 and 0.1, at BER of 10^{-4}. The result is similar to that in **Fig. 6**. Therefore, it can also be concluded that the nearest location for a relay to the destination node is the best position in a QF relay system. And it contributes to achieve the best BER performance for the proposed QF scheme in cooperative communications.

6. Conclusion

In this paper, an improved QF scheme with low order modulation and quantization is proposed with high BER performance and low complexity. The proposed 2-bit QF scheme has better performance than those of the DF scheme and the 1-bit QF ones. Then, an appropriate bit order can be chosen to achieve better performance with low complexity. Furthermore, based on the QF protocol, the optimal relay selection and power allocation are also suggested and analyzed. The numerical simulations and theoretical analyses indicated that a relay node, which is located closely to the destination node, obtains better BER performance among the QF schemes. Then, it can be applied to select the best relay position for the optimal cooperation. Finally, the achievable rate of the QF relay system is also proved to be unconstrained by the source-relay link, which surpasses that of the DF scheme. Simultaneously, higher achievable rate can be obtained by the proposed scheme in the optimal power allocation. Due to low complexity of the QF scheme, it can also be very pragmatic on the multiple relay scenarios. Besides, the short regular LDPC codes are also adopted in the improved QF scheme to enhance the good features. Particularly, the long irregular LDPC codes can be constructed and used on some occasions and they help obtain ever better BER performance along with the requirement of the multiple relay cooperation. Therefore, the proposed QF scheme is very efficient in cooperative communications with high performance and low complexity.

References

[1] Wang Xiaoxiang, Zhou Jia and Wang DongYu, "Joint relay-and-antenna selection and power allocation for AF MIMO two-way relay networks," *KSII Transactions on Internet and Information System*, vol. 10, no. 3, pp. 1016-1033, March 2016. Article (CrossRef Link).

[2] A. Sendonaris, E. Erkip, B. Aazhang, "User cooperation diversity. Part I. System description," *IEEE Transactions on Communications*, vol. 51, no. 11, pp. 1927-1938, November 2003. Article (CrossRef Link).

[3] A. Sendonaris, E. Erkip, B. Aazhang, "User cooperation diversity. Part II. Implementation aspects and performance analysis," *IEEE Transactions on Communications*, vol. 51, no. 11, pp. 1939-1948, November, 2003. Article (CrossRef Link).

[4] D. B. Da Costa, S. Aissa, "Amplify-and-forward relaying in channel-noise-assisted cooperative networks with relay selection," *IEEE Communication Letter*, vol. 14, no. 7, pp. 608-610, July, 2010. Article (CrossRef Link).

[5] H. M. Anders, J. S. Zhang, "Capacity bounds and power allocation for wireless relay channels," *IEEE Transactions on Information Theory*, vol. 51, no. 6, pp. 2020-2040, June, 2005. Article (CrossRef Link).

[6] Z. X. Liu, S. Vladimir, Z. X. Xiong, "Wyner-Ziv coding for the half-duplex relay channel," in *Proc. of IEEE International Conference on Acoustics, Speech, and Signal Processing*, vol.5, pp. 1113-1116, March 18-23, 2005. Article (CrossRef Link).

[7] A. Chakrabarti, A. Sabharwal, B. Aazhang, "Practical quantizer design for half-duplex estimate-and-forward relaying," *IEEE Transactions on Communications*, vol. 59, no. 1, pp. 74-83, January, 2011. Article (CrossRef Link).

[8] R. S. Michael, H. Q. You, "Quantize-and-forward relaying with M-ary phase shift keying," in *Proc. of IEEE Wireless Communications and Networking Conference*, pp. 42-47, March 31-April 3, 2008. Article (CrossRef Link).

[9] D. T Tran. , S. M. Sun, E. Kurniawan, "A low-complexity practical quantize-and-forward scheme for two-hop relay systems," in *Proc. of Vehicular Technology Conference (VTC Spring), Yokohama*, pp. 1-5, May 6-9, 2012. Article (CrossRef Link).

[10] Lei Liu, Ying Li, Yuping Su, and Yue Sun, "Quantize-and-forward strategy for interleave-division multiple-access relay channel," *IEEE Transactions on Vehicular Technology*, vol. 65, no. 3, pp. 1808-1814, March 2016. Article (CrossRef Link).
[11] Sha Yao, Mikael Skoglund Tùng T. Kim and H. Vincent Poor, "Half-duplex relaying based on quantize-and-forward," in *Proc. of 2011 IEEE International Symposium on Information Theory Proceedings*, pp. 2447-2451. Article (CrossRef Link).
[12] Ming Lei, Mohammad Reza Soleymani, "Diversity-multiplexing tradeoff of the half-duplex slow fading multiple-access relay channel based on generalized quantize-and-forward scheme," *IEEE Wireless Communications Letters*, vol. 4, no. 1, pp. 74-77, February, 2015. Article (CrossRef Link).
[13] R. G. Gallager, "Low-density parity-check codes," *IRE Transactions on Information Theory*, vol. 8, no. 1, pp. 21-28, January, 1962. Article (CrossRef Link).
[14] D. S. Michalopoulos, G. K. Karagiannidis, "Performance analysis of single relay selection in rayleigh fading," *IEEE Transactions on Wireless Communications*, vol. 7, no. 10, pp. 3718-3724, October, 2008. Article (CrossRef Link).
[15] Zhihang Yi, Il-Min Kim, "Diversity order analysis of the decode-and-forward cooperative networks with relay selection," *IEEE Transactions on Wireless Communications*, vol. 7, no. 5, pp. 1792-1799, May, 2008. Article (CrossRef Link).
[16] H. Eghbali, S. Muhaidat, S. A. Hejazi, et al, "Relay selection strategies for single-carrier frequency-domain equalization multi-relay cooperative networks," *IEEE Transactions on Wireless Communications*, vol. 12, no. 5, pp. 2034-2045, May, 2013. Article (CrossRef Link).
[17] Xinyi Wang, Yuanxin Sun, Huogen Yu, et al, "Outage performance analysis of amplify-and-forward cognitive relay networks with partial relay selection," in *Proc. of 2015 International Conference on Wireless Communications & Signal Processing* (WCSP), NanJing, pp. 1-5, October 15-17, 2015. Article (CrossRef Link).
[18] Zhengchuan Chen, Pingyi Fan, Dapeng Wu and Liquan Shen, "On the power allocation for hybrid DF and CF protocol with auxiliary parameter in fading relay channels," in *Proc. of 2015 IEEE Wireless Communications and Networking Conference* (WCNC 2015) - Track 1: PHY and Fundamentals, pp. 777-782, March 9-12, 2015. Article (CrossRef Link).
[19] Q. Zhang, J. M. Zhang, C. J. Shao, et al, "Power allocation for regenerative relay channel with Rayleigh fading," in *Proc. of Vehicular Technology Conference*, pp. 1167−1171, May 17-19, 2004. Article (CrossRef Link).
[20] Yaxin Xing, Yueyun Chen, Chen Lv, Zheng Gong, Ling Xu, "Swarm intelligence-based power allocation and relay selection algorithm for wireless cooperative network," *KSII Transactions on Internet and Information System*, vol. 10, no. 3, pp. 1111-1130, March, 2016. Article (CrossRef Link).
[21] Bin Zhong, Dandan Zhang and Zhongshan Zhang, "Power allocation for opportunistic full-duplex based relay selection in cooperative systems," *KSII Transactions on Internet and Information System*, vol. 9, no. 10, pp. 3908-3920, October, 2015. Article (CrossRef Link).
[22] T. S. Rappaport, *Wireless communications: principles and practice*, 2nd Edition, Prentice Hall PTR Upper Saddle River, New Jersey, 1996. Article (CrossRef Link).
[23] D. J. C. MacKay, "Good error-correcting codes based on very sparse matrices," *IEEE Transactions on Information Theory*, vol. 45, no. 2, pp. 399-431, March, 1999. Article (CrossRef Link).
[24] R. Hu, J. Li, "Practical compress-and-forward in user cooperation: Wyner-Ziv cooperation," in *Proc. of 2006 IEEE International Symposium on Information Theory*, (Seattle, WA), pp. 489-493, July 9-14, 2006. Article (CrossRef Link).
[25] Stephan ten Brink, Gerhard Kramer, and Alexei Ashikhmin, "Design of low-density parity-check codes for modulation and detection," *IEEE Transactions on Wireless Communications*,vol. 52, no. 4, pp. 670-678, April, 2004. Article (CrossRef Link).
[26] S. Yao, T. T. Kim, M. Skoglund, et al, "Half-duplex relaying over slow fading channels based on quantize-and-forward," *IEEE Transactions on Information Theory*, vol, 59, no. 2, pp. 860-872, Feburary, 2013. Article (CrossRef Link).

[27] S. Boyd, L. Vandenberghe, "Convex optimization," *Cambridge University Press*, U.K. 2003. Article (CrossRef Link).

Jianrong Bao received his B.S. degree in Polymer Materials & Eng., and the M.S.E.E. degree from Zhejiang University of Technology, Hangzhou, China, in 2000 and 2004, respectively. He received his Ph.D. E.E. degree from the Department of Electronic Engineering, Tsinghua University, Beijing, China, in 2009. Now he is with the school of Information Engineering, Hangzhou Dianzi University, Hangzhou, China. He has been an on–the-job postdoctoral researcher at the National Mobile Communications Research Laboratory, Southeast University, Nanjing, China from 2014 to 2016. And he has also visited and studied at the Department of Electrical Engineering, Columbia Univesity, as a Visiting Scholar in 2015. His research interests include space wireless communications, cooperative communications, communication signal processing and channel coding, *etc.*

Dan He received her B.S.E.E. degree from Jiangxi University of Science and Technology, Ganzhou, China, in 2013. Currently, she pursuits her M.S.E.E. degree in the school of Communication Engineering, Hangzhou Dianzi University, Hangzhou, China. Her research interests include cooperative space communications, information theory and channel coding, *etc.*

Xiaorong Xu received the B. Eng. degree in Communication Engineering and M. Eng. degree in Communication and Information System from HDU, Hangzhou, China, in 2004 and 2007, respectively. He received Ph.D. degree major in Signal and Information Processing from Nanjing University of Posts and Telecommunications (NJUPT), Nanjing, China, in 2010. Currently, he is working as a associate professor in HDU. Dr. Xu's research interests emphasize on energy efficiency in cooperative communications, energy efficiency and PHY security in Cognitive Radios (CR), as well as Compressive Sensing (CS) theory, etc.

Bin Jiang received his B.S.E.E. and the M.S.E.E. degree from Hangzhou Dianzi University, Hangzhou, China, in 1999 and 2004, respectively. He is with the school of Communication Engineering, Hangzhou Dianzi University, Hangzhou, China. He is also the Senior Experimentalist and also the Office Director of the school. His research interests mainly include modern wireless communications, communication signal processing, channel coding, information security, *etc*.

Minhong Sun received his B.S. C.S. degree from Nanchang Institute of Aeronautical Technology, Nanchang, China, in 2001. He received his M.S. E.E. degree from Chengdu University of Technology, Chengdu, China, in 2005. He received his Ph.D. E.E. degree from the School of Electronic Engineering, University of Electronic Science and Technology, Chendu, China, in 2008. He is with the school of Communication Engineering, Hangzhou Dianzi University, Hangzhou, China. He is also an on–the-job postdoctoral researcher at the School of Information Science and Engineering, Southeast University, Nanjing, China. His research interests include satellite communications and navigations, modern signal processing, channel coding, *etc*.